cleaves *Sp* phosphorothioate bonds but not *Rp* bonds (*13*), whereas SVPD shows the opposite specificity (*10*). Control experiments with chemically synthesized phosphorothioate dinucleotides showed that these enzymes cleaved with the expected stereospecificity under identical conditions (Fig. 5C). These results show that the *Sp* phosphorothioate in the substrate RNA was inverted to *Rp* in the second step of group II self-splicing.

Much has been written about the apparent similarities between the structures and splicing mechanisms of group II and pre-mRNA introns (*14*). These similarities could be due to a common evolutionary origin or due to chemical determinism driven by a need to carry out similar reactions. Our data extend the similarities to the level of the stereochemistry of the fundamental reactions of these introns and provide strong support for a close relation between these two classes of introns. Because group II intron ribozymes carry out the same chemical reactions as in pre-mRNA splicing but without the need to assemble a spliceosome from trans-acting factors, they might represent a more accessible system in which to investigate the details of these reactions.

REFERENCES AND NOTES

1. K. L. Maschhoff and R. A. Padgett, *Nucleic Acids Res.* **21**, 5456 (1993).
2. M. J. Moore and P. A. Sharp, *Nature* **365**, 364 (1993).
3. F. Eckstein, *Annu. Rev. Biochem.* **54**, 367 (1985).
4. T. A. Steitz and J. A. Steitz, *Proc. Natl. Acad. Sci. U.S.A.* **90**, 6498 (1993); M. Yarus, *FASEB J.* **7**, 31 (1993).
5. J. Rajagopal, J. A. Doudna, J. W. Szostak, *Science* **244**, 692 (1989); J. A. McSwiggen and T. R. Cech, *ibid.*, p. 679; E. Suh and R. B. Waring, *Nucleic Acids Res.* **20**, 6303 (1992).
6. P. S. Perlman, C. L. Peebles, C. Daniels, in *Intervening Sequences in Evolution and Development*, E. M. Stone and R. J. Schwartz, Eds. (Oxford Univ. Press, New York, 1990), pp. 112–161; C. Guthrie, *Science* **253**, 157 (1991).
7. K. A. Jarrell, C. L. Peebles, R. C. Dietrich, S. L. Romiti, P. S. Perlman, *J. Biol. Chem.* **263**, 3432 (1988).
8. The *Rp* phosphorothioate oligonucleotide contained 1.5% phosphodiester oligonucleotide as determined by analytical high-pressure liquid chromatography (HPLC). The level of splicing seen with the *Rp* phosphorothioate-substituted RNA is consistent with this level of purity. The final extents of the splicing reactions at 7.5 hours were *Rp*, 2 to 4%; *Sp*, 80 to 85%; and oxygen, 95 to 98%.
9. Preliminary experiments show that the reduction in the initial rate of reaction on *Sp* phosphorothioate substitution is at least 30-fold. Further experiments show that addition of $MnCl_2$ to the *Sp* reaction enhanced the rate of this reaction without affecting the rate of reaction of the unsubstituted RNA. These results suggest that one or more divalent metal ions are involved in contacts with the prochiral-Sp oxygen. Similar experiments with the *Rp* phosphorothioate-substituted RNAs at either splice junction showed no detectable reaction on addition of $MnCl_2$.
10. P. M. Burgers and F. Eckstein, *Proc. Natl. Acad. Sci. U.S.A.* **75**, 4798 (1978); P. S. Nelson, C. T. Bach, J. P. H. Verheyden, *J. Org. Chem.* **49**, 2314 (1984); A. D. Griffiths, B. V. L. Potter, I. C. Eperon, *Nucleic Acids Res.* **15**, 4145 (1987).
11. G. Gish and F. Eckstein, *Science* **240**, 1520 (1988).
12. M. Podar, P. S. Perlman, R. A. Padgett, unpublished data.
13. B. V. L. Potter, B. A. Connolly, F. Eckstein, *Biochemistry* **22**, 1369 (1983).
14. P. A. Sharp, *Cell* **42**, 397 (1985); T. R. Cech, *ibid.* **44**, 207 (1986); A. Jacquier, *Trends Biochem. Sci.* **15**, 351 (1991); A. M. Weiner, *Cell* **72**, 161 (1993).
15. Oligonucleotides containing single sites of phosphorothioate modification were synthesized, modified, and purified as described (*1*) except that the initial product was purified by HPLC on a SAX column [G. Slim and M. J. Gait, *Nucleic Acids Res.* **19**, 1183 (1991)] before reversed-phase HPLC separation of the isomers. The configurations of the separated phosphorothioate isomers were verified by comparing the products of digestion with nuclease P1, ribonuclease A, and SVPD, which have established stereospecificities for cleavage of phosphorothioates. The sequence of the 5′ splice junction oligonucleotide was 5′-UC(S)GAGCGGUCU, where (S) denotes the position of sulfur substitution. The sequence of the 3′ splice junction oligonucleotide was 5′-AU-(S)ACUAUGUAU.
16. A 68-nucleotide fragment of exon 1 ending two nucleotides before the 5′ splice junction was transcribed with T7 RNA polymerase from a polymerase chain reaction (PCR)–generated template. This was ligated to the synthetic 11-nucleotide 5′ splice junction RNA by means of DNA-mediated ligation [(*1*) and M. J. Moore and P. A. Sharp, *Science* **256**, 992 (1992)]. The ligated product was purified by preparative gel electrophoresis. To generate the complete intron RNA, we ligated this E1 + oligonucleotide RNA to a 938-nucleotide RNA beginning 10 nucleotides downstream of the 5′ splice junction and continuing through 60 nucleotides of the second exon. This RNA was made by T7 RNA polymerase transcription of a PCR-generated template, dephosphorylated with calf intestinal phosphatase, and labeled at the 5′ end with T4 polynucleotide kinase and [γ-^{32}P]adenosine triphosphate (ATP). The full-length intron RNA was purified by preparative gel electrophoresis.
17. Synthetic 11-nucleotide 3′ splice junction RNAs were 3′ end-labeled with ^{32}P pCp with T4 RNA ligase and then joined by means of DNA-mediated ligation to a T7 RNA polymerase transcript containing the 5′ exon and the entire intron ending two nucleotides before the 3′ splice junction. The ligated product was purified by preparative gel electrophoresis.
18. Splicing reactions were carried out in 0.5 M $(NH_4)_2SO_4$, 100 mM $MgCl_2$, 1 mM dithiothreitol, and 40 mM Hepes buffer (pH 7.3) at 45°C (*7*). Products were analyzed on a 4% polyacrylamide gel containing 8 M urea and quantitated on a Molecular Dynamics PhosphorImager.
19. Samples were digested with 3.3×10^{-3} units of SVPD (Type I, Sigma) in 10 mM tris-HCl (pH 8.0), 1 mM EDTA, and 5 mM Na_2PO_4 with 1 μg of tRNA for 60 min at 37°C or 20 ng of nuclease P1 in 15 mM ammonium acetate (pH 4.6) with 1 μg of tRNA for 60 min at 37°C. Iodoethanol treatment was as described (*11*), which in the absence of a free 2′ hydroxyl group results mainly in desulfurization of the phosphorothioate.
20. RNAs containing either a phosphodiester bond or an *Sp* phosphorothioate bond at the 3′ splice site and containing a single labeled phosphorus one position 5′ of the 5′ splice site were prepared as follows: an exon 1 RNA ending at position −1 was ligated to a 5′ ^{32}P-labeled RNA transcript of the entire intron initiated with CpG, which ended at position −2 from the 3′ splice site. This labeled RNA was then ligated to either the control oxygen, *Rp* phosphorothioate, or *Sp* phosphorothioate 3′ splice site oligonucleotide. These RNAs were spliced and digested with nuclease P1 or SVPD as above.

21. Supported by NIH grants GM31480 (P.S.P.) and GM45371 (R.A.P.) and Welch Foundation grants I-1211 (P.S.P.) and I-1035 (R.A.P.).

3 August 1994; accepted 18 October 1994

Polyglycylation of Tubulin: A Posttranslational Modification in Axonemal Microtubules

Virginie Redeker, Nicolette Levilliers, Jean-Marie Schmitter, Jean-Pierre Le Caer, Jean Rossier,* André Adoutte, Marie-Hélène Bré

A posttranslational modification was detected in the carboxyl-terminal region of axonemal tubulin from *Paramecium*. Tubulin carboxyl-terminal peptides were isolated and analyzed by Edman degradation sequencing, mass spectrometry, and amino acid analysis. All of the peptides, derived from both α and β tubulin subunits, were modified by polyglycylation, containing up to 34 glycyl units covalently bound to the γ carboxyl group of glutamyl residues. This modification, present in one of the most stable microtubular systems, may influence microtubule stability or axoneme function, or both.

The axoneme of cilia and flagella comprises a bundle of microtubules typically arranged as a ring of nine doublets around a pair of single microtubules. This structure is among the most stable microtubular assemblies known and contains >150 different proteins, of which α and β tubulins are the most abundant (*1*). Immunocytochemical and immunoblotting studies with antibodies to *Paramecium* axonemal tubulin—polyclonal anti-PA tubulin and monoclonal AXO 49, which show similar specificities—suggest that axonemal tubulin undergoes a posttranslational modification (*2*, *3*). The reactive epitope (i) appears late in the assembly of stable microtubules, (ii) is located in the COOH-terminal domain of both α

V. Redeker, J.-P. Le Caer, J. Rossier, Institut Alfred Fessard, CNRS Unité Propre de Recherche 2212, 91198 Gif-sur-Yvette Cedex, France.
N. Levilliers, A. Adoutte, M.-H. Bré, Laboratoire de Biologie Cellulaire 4, CNRS Unité de Recherche Associée 1134, Université Paris XI, 91405 Orsay Cedex, France.
J.-M. Schmitter, Laboratoire de Biochimie, CNRS Unité de Recherche Associée 240, Ecole Polytechnique, 91128 Palaiseau Cedex, France.
*To whom correspondence should be addressed.

and β tubulin, and (iii) is distinct from other reported posttranslational modifications (detyrosylation, phosphorylation, and glutamylation). This epitope, originally observed in *Paramecium* axonemes, is also detected in cilia and flagella both from protists and metazoa, including an array of invertebrates and vertebrates (*2*, *3*).

To characterize the nature of this modification, we used *Paramecium* axonemal tubulin because it reacts strongly with the AXO 49 antibody and is likely to be enriched in the modification. *Paramecium* axonemal tubulin was extracted from cilia as described (*4*) and digested with endoproteinase Asp-N (*5*). Both α and β tubulin sequences possess an Asp-N cleavage site close to the COOH-terminus (*6*). Digestion products were separated by high-performance liquid chromatography (HPLC) on a DEAE anion-exchange column (Fig. 1), which allowed us to recover COOH-terminal peptides from both α and β tubulin in the most acidic fractions, corresponding to the later phase of the elution profile. Each of these acidic fractions was further purified by HPLC on a C_8-RP300 reversed-phase column, and two major peaks were consistently obtained (*7*). These peaks were subsequently analyzed by amino acid sequencing and mass spectrometry.

Automatic Edman degradation showed that the two major species separated by each reversed-phase elution apparently corresponded to the 16 COOH-terminal amino acids of β1 tubulin and the 26 COOH-terminal amino acids of α1 and α2 tubulin (*7*). However, in 20 Edman degradations, we did not detect any signal corresponding to Glu^{437} in β tubulin or to Glu^{445} in α tubulin. Polyglutamylation of brain tubulin was discovered as a result of a similar gap in the amino acid sequence (*8*).

To identify the nature of the modification of the axonemal tubulins, we further characterized each of the isolated peptides. Matrix-assisted laser desorption ionization–time of flight–mass spectrometry (MALDI-TOF-MS) analysis showed that each fraction, apparently homogeneous on reversed-phase HPLC, was in fact heterogeneous and produced several molecular ions whose masses differed by increments of multiple units of 57 daltons (Fig. 2). This value corresponds to the mass of a glycyl residue. The identification of the added units as glycyl residues was confirmed by total amino acid composition analysis of α and β tubulin COOH-terminal peptides emerging from the reversed-phase column (*9*).

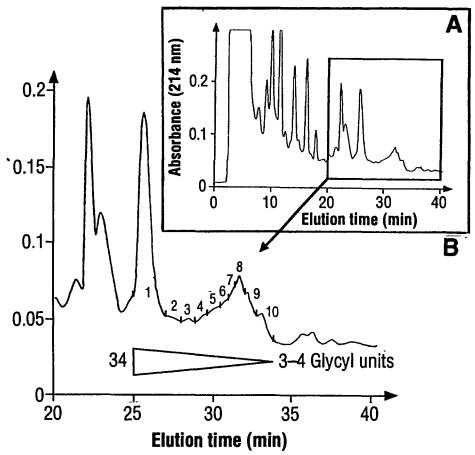

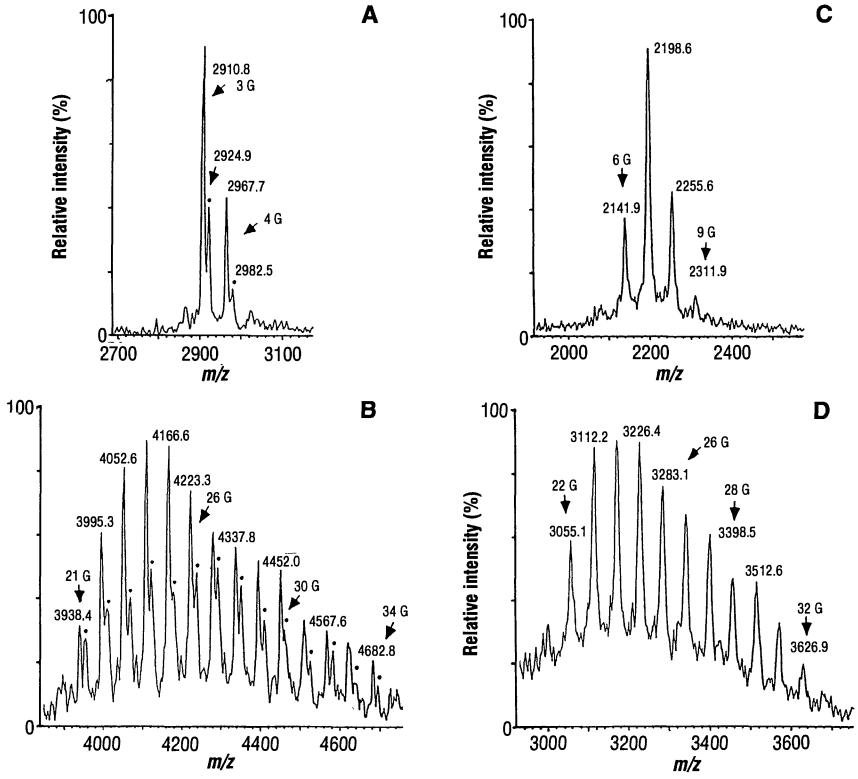

Fig. 1 (left). Purification of the COOH-terminal peptides generated by endoproteinase Asp-N digestion of *Paramecium* axonemal tubulin. *Paramecium* ciliary axonemes were isolated by selective detachment of cilia from the cell bodies (induced by $MnCl_2$), and tubulin was extracted by sonication of microtubule doublets (*4*). Purified tubulin (1 mg) was digested for 6 hours at 36°C with endoproteinase Asp-N (2.5 μg) in 430 μl of 50 mM tris-HCl (pH 8.0) (*5*). Digestion was terminated by placing the samples at −80°C. The peptide mixture was separated by HPLC on an anion-exchange column (DEAE 5PW; Waters); elution was performed at a flow rate of 1 ml/min with a linear gradient from 50 to 500 mM NaCl in 20 mM tris-HCl (pH 8.0) over 60 min. The absorbance of the eluted peptides was monitored at 214 nm. (**A**) The complete chromatogram. (**B**) Enlarged region of the chromatogram in which the COOH-terminal acidic peptides were eluted (*19*, *31*). The acidic peptides eluted from the column between 25 and 34 min, denoted 1 to 10, were collected and further purified by reversed-phase HPLC (*7*). **Fig. 2 (right).** MALDI-TOF-MS analysis of COOH-terminal peptides of *Paramecium* axonemal α and β tubulin. Analysis of peptides purified from peaks 1 and 8 from the DEAE column was performed on a VG Analytical Tofspec mass spectrometer equipped with a 337-nm laser, with a 25-kV acceleration voltage (*32*). From 50 to 100 shots were accumulated for each spectrum acquisition in the positive-ion mode. Average mass to charge (*m/z*) ratios of the protonated molecular ions (MH^+) are indicated on the spectra. (**A** and **B**) Analysis of α tubulin peptides from peaks 8 and 1, respectively. For the COOH-terminal peptides of α1 tubulin (calculated MH^+ mass of 2740.8 daltons, corresponding to the sequence ^{424}DLAALEKDYEEVGIETAEGEGEEGEG^{449}) and α2 tubulin (calculated MH^+ mass of 2754.8 daltons, corresponding to the sequence ^{424}DLAALEKDYEEVGIETAEGEGEEGEA^{449}), the number of additional glycyl units (57.05 daltons) was determined from the differences between the mass values obtained and the calculated mass value of the unmodified peptide. The first mass signals (A) correspond to the unmodified peptides of α1(424–449) and α2(424–449) carrying three glycyl units [2911.9 daltons = 2740.8 + (3 × 57.05), and 2925.9 daltons = 2754.8 + (3 × 57.05), respectively]. The other mass signals represent additions of up to 34 glycyl units (B). The molecular ions corresponding to isotype α2 are designated by dots. (**C** and **D**) Analysis of β tubulin peptides from peaks 8 and 1, respectively. The calculated MH^+ mass of the unmodified COOH-terminal peptide of β tubulin (corresponding to the sequence ^{427}DATAEEEGEFEEEGEQ^{442}) was 1799.7 daltons. The highest mass signal observed represents the addition of up to 32 glycyl units [3625.3 daltons = 1799.7 + (32 × 57.05)] (D). The difference between the calculated average mass and the experimental mass determination shown (0.1 to 1.6 daltons) is consistent with the accuracy of MALDI-TOF-MS.

Spectra corresponding to one of the lowest (Fig. 2, A and C) and one of the highest (Fig. 2, B and D) amounts of glycylation are shown for α and β tubulin, respectively. The molecular ions obtained for the β tubulin peptides corresponded to the theoretical mass of the COOH-terminal β tubulin peptide (from Asp^{427}) bearing 4 to 32 added units of 57 daltons. One of the most acidic peaks (denoted 8) from the DEAE column (Fig. 1) contained six to nine added glycyl units, (Fig. 2C), whereas a less acidic peak (denoted 1) contained 22 to 32 added glycyl units (Fig. 2D). Each intermediate amount of glycylation (from 4 to 32 added glycyl units) was observed.

The mass signals observed for α tubulin corresponded to the calculated mass of the COOH-terminal α tubulin peptide (from Asp^{424}) bearing 3 to 34 added units of 57 daltons (Fig. 2, A and B). Two molecular ions differing by 14 daltons within each increment of 57 daltons were also detected. This value of 14 daltons corresponds to the difference between the masses of Gly and Ala, which are the terminal residues of α1 and α2 tubulin isotypes, respectively.

Thus, both α and β tubulin were modified by the addition of 3 to 34 glycyl units to the COOH-terminal tail. Among the peaks analyzed, we did not observe any unmodified COOH-terminal tubulin peptides, nor any COOH-terminal peptides bearing glutamyl units. Indeed, the amount of glutamylated tubulin appears to be low in the *Paramecium* axoneme (*10*).

By analogy with the discovery of polyglutamylation of tubulin (*8*), we propose that the glycyl units are added to the first residue undetected by Edman degradation: Glu^{437} for β tubulin and Glu^{445} for α tubulin. However, we could not exclude the possibility that glycyl units are linked to other COOH-terminal glutamyl residues (Glu^{438}, Glu^{439}, and Glu^{441} for β tubulin, and Glu^{446} and Glu^{448} for α tubulin). To identify the location of the lateral glycyl chain, we digested axonemal tubulin with thermolysin (*11*), which yields smaller peptides than those obtained by digestion with endoproteinase Asp-N. Separation of the digestion products on a DEAE column revealed one major acidic peptide, which was characterized by automatic Edman degradation and fragmentation by electrospray–mass spectrometry analysis (*12*). We obtained the amino acid sequence FXE (where X is any amino acid) (*13*), whereas the mass was that of a tetrapeptide, F,E,E,G. Fragmentation analysis revealed that the peptide corresponded to $^{436}FEE^{438}$ from β tubulin in which Glu^{437} was modified by the addition of a glycine residue (*12*). Although this observation is consistent with the modification of Glu^{437}, rather than Glu^{438}, on β tubulin, we still cannot exclude the presence of other glycylation sites.

As far as we are aware, the polyglycylation modification has not been described for any other protein. The length of the peptide chain generated by the addition of glycyl residues is the longest non–genetically coded amino acid addition identified. Numerous posttranslational modifications affect α and β tubulin subunits. Most of these modifications were detected initially in the brain, where tubulin heterogeneity is particularly high. α Tubulin undergoes acetylation of Lys^{40} (*14*), reversible removal of the COOH-terminal Tyr^{451} (*15*), removal of the penultimate Glu^{450} (*16*), and glutamylation of Glu^{445} (*8*); whereas β tubulin is modified by phosphorylation of Ser^{444} and Tyr^{437} in the βIII isotype (*17*) and Ser^{441} in the βVI isotype from the marginal band of erythrocytes (*18*), and glutamylation of Glu^{438} in βIII (*17*), Glu^{435} in βII (*19*, *20*), Glu^{434} in βIVa, and Glu^{441} in βI (*21*) isotypes. Except for acetylation, all of these modifications, which contribute to the diversity of microtubule subsets within the cell (*22*), concern the 10 COOH-terminal residues of α and β tubulin.

Polyglycylation was chemically characterized on ciliary axonemal tubulin from *Paramecium*. Fractions from the DEAE column (Fig. 1) were examined by dot-blot analysis (*23*) with the monoclonal antibody AXO 49, which decorates the stable microtubule arrays in *Paramecium* (*3*). The greatest reactivity was observed in fractions 1 to 3, corresponding to the highly glycylated forms of tubulin (containing 11 to 34 and 15 to 32 added glycyl units for the α and β subunits, respectively). AXO 49 recognizes tubulin from axonemes (ciliary and flagellar) from a wide variety of species, extending from protozoa to metazoa. For example, immunoreactivity was detected in ciliates as diverse as *Euplotes*, *Stylonychia*, and *Tetrahymena*, which are as distant, in molecular terms, as plants are from animals, as well as in a wide array of invertebrates and vertebrates, including sea urchin (spermatozoa) and quail (oviduct cilia) (*2*, *3*). Polyglycylation may therefore be a general modification of axonemal tubulin of both protozoa and metazoa.

In most instances, microtubule stability correlates with the presence of posttranslational modifications. Detyrosylation and acetylation, for example, are generally absent from most newly formed microtubules and are more prevalent on stabilized and aging microtubules (*24*, *25*). However, these modifications are probably the consequence of microtubule stability rather than its cause (*25*). All of the microtubules decorated by AXO 49 belong to a stable class that is unaffected by cold or nocodazole treatment (*26*). Thus, polyglycylation appears to be associated with stable microtubule arrays.

The importance of the COOH-terminal domain of tubulin for the structural organization of axonemal microtubules is manifested by the observation that axonemes from spermatozoa of *Drosophila* expressing a truncated testis-specific β2 tubulin (devoid of the last 15 amino acids) fail to assemble into a structure that resembles the canonical "9+2" microtubule array with its associated membrane (*27*). In addition, the COOH-terminal domain of tubulin, which is exposed as a flexible, accessible arm on the surface of the microtubule lattice, has been suggested to mediate interactions with other molecules, such as microtubule-associated proteins (MAPs) (*28*). Removal of the COOH-terminal region of the molecule, or chemical neutralization of the COOH-terminal acidic groups by amidation, promotes tubulin assembly into microtubules and inhibits interactions with MAPs (*29*). The elution profile obtained during DEAE chromatography of tubulin peptides released after endoproteinase Asp-N digestion showed that the highly glycylated peptides eluted earlier than the less glycylated ones (Fig. 1). Thus, polyglycylation in the COOH-terminal domain of tubulin appears to decrease the acidity of this region of the molecule. By changing the net charge and hydrophilicity of the tubulin COOH-terminus, polyglycylation may thus favor microtubule assembly. Moreover, the diversity of polyglycyl chain length may serve to modulate interactions between microtubules and MAPs along the axonemes.

Bridges and "moving rafts" connecting the axonemal microtubules and the membrane have been visualized as opaque structures in electron micrographs of cilia and flagella, and may be important in intraflagellar transport (*30*). Because immunocytochemical studies have shown that AXO 49 immunoreactivity is exclusively localized over stable microtubules in the proximity of membranous structures (*2*, *26*), the additional glycyl chains may anchor axonemal microtubules to the membranes and participate in their stabilization and in axoneme function.

REFERENCES AND NOTES

1. G. Piperno, B. Huang, D. J. L. Luck, *Proc. Natl. Acad. Sci. U.S.A.* **74**, 1600 (1977); A. Adoutte *et al.*, *J. Cell Biol.* **86**, 717 (1980).
2. A. Adoutte, M. Claisse, R. Maunoury, J. Beisson, *J. Mol. Evol.* **22**, 220 (1985); A. Adoutte *et al.*, *Biol. Cell* **71**, 227 (1991).
3. A. M. Callen *et al.*, *Biol. Cell*, in press; N. Levilliers *et al.*, unpublished data.
4. G. Geuens, A. M. Hill, N. Levilliers, A. Adoutte, M. DeBradander, *J. Cell Biol.* **108**, 939 (1989).
5. U. Geuβ, M. Schäffer, J. Tschakert, S. Fischer, G.-B. Kresse, *J. Protein Chem.* **9**, 299 (1990).
6. Four α and three β tubulin genes have been identified, of which two α (α1 and α2) and one β (β1) have been sequenced [P. Dupuis, *EMBO J.* **11**, 3713 (1992); ———, thesis, Université Paris XI (1992)].
7. The fractions collected from the DEAE column were injected onto a reversed-phase column (Aquapore RP-300; 7 μm, 220 by 2.1 mm) and peptides were eluted with solvents A (0.1% trifluoroacetic acid) and

B (80% acetonitrile and 0.09% trifluoroacetic acid). Solvent B was maintained at 1% for 10 min and the following gradient was then applied at a flow rate of 200 μl/min: Solvent B was linearly increased from 1 to 10% in 1 min, from 10 to 20% in 30 min, from 20 to 30% in 10 min, from 30 to 40% in 20 min, and from 40 to 100% in 10 min. Most of the fractions denoted 1 to 10 from the DEAE column yielded three peaks by reversed-phase separation. Edman degradation sequencing revealed that the two major peaks, which eluted between 16 and 17% and between 35 and 36% solvent B, corresponded, respectively, to β and α tubulin COOH-terminal peptides. The β tubulin peptide (^{427}DATAEEEGEF^{436}. . .) corresponded to the predicted cleavage site for endoproteinase Asp-N, whereas the major α tubulin peptide (^{424}DLAALE-KDYEEVGIETAEGEG^{444}. . .) resulted from incomplete cleavage in the COOH-terminal domain. The minor peak, which eluted between 20 and 24% solvent B, corresponded to the COOH-terminal peptide of α tubulin generated by complete digestion (^{431}DYEEVGIETAEGEG^{444}. . .). The most acidic fractions that eluted after 34 min from the DEAE column were also purified by reversed-phase HPLC; determination of their amino acid sequences showed that they corresponded to internal acidic sequences of the α and β tubulin subunits.

8. B. Eddé *et al.*, *Science* **247**, 83 (1990).
9. Amino acid composition was determined with an Applied Biosystems amino acid analyzer (model 420). Derivatization was achieved with phenylisothiocyanate and the hydrolysis was performed on-line. The results confirmed both the presence of the different amino acids contained in the sequences of the tubulin peptides and the variation of the composition in glycyl residues. For example, for the α(424–449) tubulin peptides, the molar ratio of Tyr to Thr (1:1) was constant, whereas the molar ratio of Gly to Thr was significantly higher (8:1 and 13:1 for the peaks denoted 8 and 3, respectively, from the DEAE separation) than the values expected (4:1 or 5:1) for the unmodified peptides (α2 or α1, respectively). For the β(427–442) tubulin peptides, the molar ratio of Asp to Thr (1:1) was constant, whereas the molar ratio of Gly to Thr was significantly higher (8:1 and 14:1 for the peaks denoted 8 and 3, respectively, from the DEAE separation) than the value expected (2:1) for the unmodified peptide.
10. M.-H. Bré, B. DeNéchaud, A. Wolff, A. Fleury, *Cell Motil. Cytoskel.* **27**, 327 (1994).
11. H. Matsubara, *Methods Enzymol.* **19**, 642 (1970).
12. The sequence (FXE) of the major peptide matched that of ^{436}FEE^{438} of β tubulin (X indicates the presence of a gap in the sequence because at that cycle no derivatized amino acid was identified) (*13*). The protonated molecular ion (MH^+) observed by electrospray–mass spectrometry had a mass of 481.0 daltons, corresponding to that of a tetrapeptide composed of one Phe, one Gly, and two Glu residues. Fragmentation of this tetrapeptide confirmed that, according to the amino acid sequence deduced from the corresponding nucleotide sequence, the fragments observed (334.0, 317.0, and 306.0 daltons) could be derived only from the peptide ^{436}FEE^{438} in which Glu^{437} was modified by the addition of one Gly residue. The amino acid analysis also confirmed the addition of one glycyl residue. These results suggest the presence of at least one major glycylation site on Glu^{437} of β tubulin. Thermolysin cleaved the lateral polyglycylated chain, possibly as a result of the broad specificity of this enzyme (*11*), which can cleave peptide bonds at the NH_2-terminal end of glycyl residues. Such peptide bonds present in the polyglycylated chain could be readily cleaved, given that the hydrophobic character of the bulky lateral chain is favorable for recognition by the endoproteinase. After thermolysin digestion, we did not detect any modified α tubulin peptides in the later phase of the DEAE elution profile. Such peptides may have eluted earlier if they were longer and less acidic than those obtained from β tubulin. Molecular mass determination of 50 pmol of peptide was performed on a Trio 2000 mass spectrometer with an electrospray ion source and a quadrupole mass analyzer (VG Biotech, Manchester, UK). The carrier solvent was 50% acetonitrile, 49% water, and 1% formic acid. Fragmentation was obtained by increasing the voltage cone to 70 V.
13. Single-letter abbreviations for the amino acid residues are as follows: A, Ala; D, Asp; E, Glu; F, Phe; G, Gly; I, Ile; K, Lys; L, Leu; M, Met; Q, Gln; R, Arg; T, Thr; V, Val; W, Trp; and Y, Tyr.
14. M. LeDizet and G. Piperno, *Proc. Natl. Acad. Sci. U.S.A.* **84**, 5720 (1987).
15. D. Raybin and M. Flavin, *J. Cell Biol.* **73**, 492 (1977).
16. L. Paturle-Lafanechère *et al.*, *Biochemistry* **30**, 10523 (1991).
17. J. E. Alexander *et al.*, *Proc. Natl. Acad. Sci. U.S.A.* **88**, 4685 (1991).
18. M. Rüdiger and K. Weber, *Eur. J. Biochem.* **218**, 107 (1993).
19. V. Redeker, R. Melki, D. Promé, J.-P. Le Caer, J. Rossier, *FEBS Lett.* **313**, 185 (1992).
20. M. Rüdiger, U. Plessman, K. D. Klöppel, J. Wehland, K. Weber, *ibid.* **308**, 101 (1992).
21. J. Mary, V. Redeker, J.-P. Le Caer, J. C. Promé, J. Rossier, *ibid.* **353**, 89 (1994).
22. K. Greer and J. L. Rosenbaum, in *Cell Movement*, F. D. Warner and J. R. McIntosh, Eds. (Liss, New York, 1989), vol. 2, pp. 47–66.
23. B. Canas, Z. Dai, H. Lackand, R. Poretz, S. Stein, *Anal. Biochem.* **211**, 179 (1993).
24. J. C. Bulinski, J. E. Richards, G. Piperno, *J. Cell Biol.* **106**, 1213 (1988); E. Schulze, D. J. Asai, J. C. Bulinsky, M. Kirschner, *ibid.* **105**, 1020 (1987).
25. M.-H. Bré, T. E. Kreis, E. Karsenti, *ibid.* **105**, 1283 (1987); S. Khawaja, G. G. Gundersen, J. C. Bulinski, *ibid.* **106**, 2167 (1988); J. Wehland and K. Weber, *J. Cell Sci.* **88**, 185 (1987).
26. A. Fleury *et al.*, unpublished data.
27. J. D. Fackenthal, F. R. Turner, E. C. Raff, *Dev. Biol.* **158**, 213 (1993).
28. L. Serrano, J. Avila, R. B. Maccioni, *Biochemistry* **23**, 4675 (1984); D. L. Sackett, D. A. Zimmerman, J. Wolff, *ibid.* **28**, 2662 (1989); H. Hagiwara, H. Yorifuji, R. Sato-Yoshitake, N. Hirokawa, *J. Biol. Chem.* **269**, 3581 (1994).
29. L. Serrano, J. de la Torre, R. B. Maccioni, J. Avila, *Proc. Natl. Acad. Sci. U.S.A.* **81**, 5989 (1984); R. Melki, P. Kerjan, J. P. Waller, M. F. Carlier, D. Pantaloni, *Biochemistry* **30**, 11536 (1991); M. Mejillano and R. H. Himes, *J. Biol. Chem.* **266**, 657 (1991).
30. W. L. Dentler, in *Ciliary and Flagellar Membranes*, R. A. Bloodgood, Ed. (Plenum, New York, 1990), pp. 31–64; K. Johnson and J. Rosenbaum, *Trends Cell Biol.* **3**, 156 (1993).
31. V. Redeker, J.-P. Le Caer, J. Rossier, J. C. Promé, *J. Biol. Chem.* **266**, 23461 (1991).
32. Samples were prepared by mixing 1.5 μl of matrix (saturated solution of α-cyano-4-hydroxycinnamic acid in 40% acetonitrile and 0.1% trifluoroacetic acid) with 1 μl of the peptide in 0.1% trifluoroacetic acid (1 to 4 pmol), applying to the stainless steel target, and drying at room temperature. The external standards used for calibration were the hexapeptide LMWRFA and bovine insulin.
33. We thank F. Iftode for help with *Paramecium* cultures, D. Faucher for help with amino acid analysis, B. Monegier from Rhône Poulenc Rorer (Vitry, France) for confirmation of the structure of the branched tetrapeptide by mass spectrometry analysis, and J. Beisson, A. Beaumont, and R. Melki for helpful discussions and critical reading of the manuscript. Supported by the Association pour la Recherche contre le Cancer (ARC, France), the Institut National de la Santé et de la Recherche Médicale (INSERM CRE/930808), and a predoctoral fellowship (V.R.) from la LIGUE Nationale contre le Cancer (France).

24 June 1994; accepted 23 September 1994

Evolutionary History of the Symbiosis Between Fungus-Growing Ants and Their Fungi

Ignacio H. Chapela,* Stephen A. Rehner,* Ted R. Schultz, Ulrich G. Mueller†

The evolutionary history of the symbiosis between fungus-growing ants (Attini) and their fungi was elucidated by comparing phylogenies of both symbionts. The fungal phylogeny based on cladistic analyses of nuclear 28S ribosomal DNA indicates that, in contrast with the monophyly of the ants, the attine fungi are polyphyletic. Most cultivated fungi belong to the basidiomycete family Lepiotaceae; however, one ant genus, *Apterostigma*, has acquired a distantly related basidiomycete lineage. Phylogenetic patterns suggest that some primitive attines may have repeatedly acquired lepiotaceous symbionts. In contrast, the most derived attines have clonally propagated the same fungal lineage for at least 23 million years.

Mutualistic symbioses between distantly related organisms have generated major innovations in the evolution of organic complexity, including the endocytotic organelles of the eukaryotic cell, the plant and fungal symbionts in mycorrhizae, and the ubiquitous nitrogen-fixing bacteria present in plants, animals, fungi, and protists (*1*). The reconstruction of the evolutionary history of such symbioses requires explicit phylogenies for both symbionts, a necessity that has limited the number of such studies to date (*2*). Here we report the results of a phylogenetic analysis of the attine ant–fungus symbiosis, an ancient and successful association that has culminated in the leaf-cutting ants, the dominant herbivores of the Neotropics (*3*).

All of the approximately 200 species of ants in the tribe Attini cultivate fungus gardens on which they are obligately depen-

I. H. Chapela, Systematic Botany and Mycology Laboratory, U.S. Department of Agriculture, Beltsville, MD 20705, USA, and Section of Neurobiology and Behavior, Cornell University, Ithaca, NY 14853, USA.
S. A. Rehner, Systematic Botany and Mycology Laboratory, U.S. Department of Agriculture, Beltsville, MD 20705, USA.
T. R. Schultz, Department of Entomology, Cornell University, Ithaca, NY 14853, USA.
U. G. Mueller, Section of Neurobiology and Behavior, Cornell University, Ithaca, NY 14853, USA.

*The order of the first two authors is arbitrary.
†To whom correspondence should be addressed.